

PRODUCTION AND CHARACTERISATION OF BIODEGRADABLE PLA NANOPARTICLES LOADED WITH THYMOL TO IMPROVE ITS ANTIMICROBIAL EFFECT

Ismael Marcet, Shihan Weng, Sara Sáez, Manuel Rendueles* & Mario Díaz.

Department of Chemical and Environmental Engineering, University of Oviedo, C/ Julián Clavería 8, 33006 Oviedo, Spain

* Corresponding author. Department of Chemical and Environmental Engineering, University of Oviedo, C/ Julián Clavería 8, 33006 Oviedo, Spain. Email: mrenduel@uniovi.es

Highlights

- PLA nanoparticles loaded with Thymol were prepared for the first time.
- The PLA was found to be the key variable in optimizing the nanoparticle preparation.
- The nanoparticles exhibited a high storage stability over a wide range of pHs.
- The antimicrobial activity of the nanoparticles was tested on apple pieces.

Abstract

Thymol is widely recognised as an antibacterial compound. However, its use in food technology is hindered by its high volatility, its light sensitivity and its low solubility in water. To overcome these drawbacks, the preparation of nanoparticles using polylactic acid (PLA) is proposed in this study.

The average size of the nanoparticles and thymol encapsulation efficiency parameters were studied using different PLA and thymol concentrations. Furthermore, the morphology, the storage stability of the nanoparticles at several pHs and the *in vitro* thymol release profile were also studied, as well as their thermal degradation profile. Finally, their antimicrobial activity on a real food model was measured, using for this purpose apple pieces previously inoculated with *E. coli*.

The PLA was found to be the key variable in optimizing the nanoparticle preparation, producing spherical nanoparticles with a thymol encapsulation efficiency of $60.3 \pm 8\%$. These nanoparticles showed a high storage stability at several pHs and improved antimicrobial properties in comparison with the non-encapsulated thymol.

Keywords

PLA; thymol; encapsulation; nanoparticles; antimicrobial properties; storage stability; thermal degradation; release profile.

1. Introduction

36 The aromatic and medicinal properties of the plants of the genus *Thymus* have been widely
37 recognized. These plants are usually used to make tea, as a flavouring agent and for medicinal
38 purposes (Stahl-Biskup and Sáez, 2003). The results reported reveal that the main constituent
39 obtained from the aerial parts of the plant are geraniol, linalool, gamma-terpineol, carvacrol and
40 thymol (Piccaglia et al., 1993). Thymol (2-isopropyl-5-methylphenol) is a volatile compound
41 which is a phenolic derivate of the terpene 3-hidroxy-p-cymene and its production by the plant
42 is associated with part of its defensive strategy against phytopathogenic microorganisms.
43 Numerous studies have reported the antibacterial and fungicidal properties of thymol (Andrade-
44 Ochoa et al., 2015; Džamić et al., 2015; Hernández-Hernández et al., 2014). For this reason, this
45 compound has received the attention of the food industry, thymol having been used as an
46 antimicrobial agent and authorized by the Food and Drugs Administration (FDA) of the USA as
47 generally recognised as safe (GRAS). However, there are technical limitations which hinder its
48 use, such as the high volatility of thymol at room temperature, its high light sensibility and its
49 low solubility in water (Mastelić et al., 2004).

50 One way to overcome these problems is the preparation of nanoparticles which contain thymol.
51 In the form of nanoparticles, the amount of thymol introduced into the food matrix could be
52 increased above its solubility limit, since the Brownian movement of the nanoparticles prevents
53 their sedimentation in the lower layers of the food (Huang, 2012). Furthermore, the high
54 surface-area ratio of nanoparticles enhances their contact with the microorganisms, and the
55 protective environment provided could limit the volatility of the thymol and its light-induced
56 degradation. For this reason, several authors have prepared protein-based nanoparticles which
57 incorporate thymol. To prepare these nanoparticles, the main protein used was zein, since both
58 zein and thymol are soluble in ethanol and the particles can be prepared by antisolvent
59 precipitation (Rosa et al. (2015), Li et al. (2012), Zhang et al. (2014) and Chen et al. (2015)).
60 However, the use of biodegradable synthetic polymers instead of proteins to encapsulate
61 thymol remains unstudied, although their use to prepare nanoparticles is a topic that has
62 received a lot of attention from the scientific community. These synthetic polymers have some
63 advantages with respect to proteins: they are produced with a high level of purity, the
64 experiments investigating their use have excellent reproducibility and they do not produce any
65 antigenic effect (Nair and Laurencin, 2005). In particular, polylactic acid (PLA) has been widely
66 used in biomedicine and it is considered a good material to prepare micro and nanoparticles,
67 since the particle size and shape can be controlled so as to satisfy the preparation requirements.
68 Furthermore, in this type of nanoparticle, the active agent is usually homogeneously dispersed
69 within the PLA matrix, which is positively related to the appropriate liberation of the active agent
70 (Lee et al., 2016).

71 To the best of our knowledge, this study documents the first preparation of PLA nanoparticles
72 containing thymol. The production of these nanoparticles was evaluated using different PLA and

73 thymol concentrations, and then they were characterised by evaluating their morphology,
74 encapsulation efficiency, stability at several pHs and thermal degradation profile. The
75 antimicrobial properties of the nanoparticles obtained were tested on apple pieces previously
76 inoculated with *E. coli*.

77

78 **2. Materials and methods**

79 **2.1. Materials**

80 The PLA (180 kDa) was produced by NatureWorks (4032D). The following reagents were
81 acquired in Sigma-Aldrich (St Louis, USA): thymol (ref. T0501), dichloromethane (DCM, ref
82 270997), polyvinyl alcohol (PVA, ref P8136), buffer Trizma® pH 7.0 (ref. T1819), 2,2-diphenyl-1-
83 picrylhydrazyl (DPPH, ref. D9132) and Nutrient Broth (NB, ref. 70149NB). The agar was acquired
84 in VWR (Pensilvania, USA).

85 **2.2. Preparation of PLA nanoparticles**

86 Nanoparticles were prepared following the single emulsion preparation technique (Lee et al.,
87 2016) with slight modifications: a 1% PVA solution was prepared and saturated with thymol. In
88 order to prepare this solution, the PVA at the required concentration was heated in a water bath
89 at 90 °C until it was completely dissolved. This solution was cooled to room temperature, 2
90 mg/mL of thymol was added and the mixture was stirred overnight. Then, the solution was
91 filtered to remove the non-solubilised thymol using a vacuum pump and N°1 Whatman paper.
92 The filtration process was repeated twice.

93 Three different amounts of PLA were dissolved in 7.5 mL of DCM, and for each of these PLA
94 concentrations, three different amounts of thymol were dissolved in the same DCM volume.
95 These percentages of thymol with respect to the weight of PLA, as well as the precise amounts
96 of thymol and PLA tested in each case are shown in Table 1.

97 Table 1. Amounts of PLA and thymol dissolved in the organic phase and tested to optimize the
98 nanoparticle preparation.

	Thymol		
PLA	66%	100%	133%
100 mg	66 mg	100 mg	133 mg
150 mg	100 mg	150 mg	200 mg
200 mg	133 mg	200 mg	266 mg

99

100 This DCM solution was carefully poured into 30 mL of the previously prepared PVA solution. The
101 mixture was ultrasonicated for 2.5 minutes using the Sonopuls HD 2070 system (Bandelin,
102 Germany) and the MS 73 probe, at a frequency of 20 kHz and applying a sonication amplitude
103 of 90% (100% corresponds to 212 μm). This sonication amplitude corresponds to an ultrasonic
104 intensity of 80 W/cm^2 . During the sonication process, the sample was kept in ice to avoid
105 temperature increase. To remove the DCM contained in the preparation, the emulsified solution
106 was kept in a low-pressure medium at 40 $^{\circ}\text{C}$ for 40 minutes using a rotavapor (Büchi R-205, Büchi
107 Labortechnik, Essen, Alemania). During the DCM evaporation, part of the thymol was able to
108 pass from the nanoparticles to the PVA medium. It was precisely to avert this problem that the
109 PVA solution was saturated with thymol, as was described previously.

110 After the DCM evaporation, the sample was centrifuged at 13000 rpm for 20 minutes to
111 precipitate the nanoparticles. The supernatant, which contains the PVA and is saturated with
112 thymol, was removed by decantation and it could be reused to prepare new nanoparticles. The
113 same volume of distilled water was added to the sediment, and the nanoparticles were
114 resuspended and centrifuged again at 4000 rpm for 5 minutes. In this case, the sediment was
115 discarded to remove PLA aggregates, the nanoparticles remaining in suspension.

116 **2.3. Nanoparticle size measurement and thymol content**

117 The average size of the nanoparticles and their polydispersion index (PDI) were measured using
118 dynamic light scattering (DLS, Nanosizer ZS, Malvern, UK).

119 The amount of thymol encapsulated was measured as follows: the nanoparticle suspension was
120 centrifuged at 13000 rpm for 20 minutes and the supernatant was removed and replaced with
121 the same volume of ethanol (96 $^{\circ}$). The sediment, which contains the nanoparticles, was
122 dispersed in the ethanol with the aid of the sonicator system. Then, the sample was centrifuged
123 again at 13000 rpm for 20 minutes. During this process and due to the high solubility of thymol
124 in ethanol, the active agent was extracted from the nanoparticles. Finally, 0.1 mL of this
125 ethanolic solution was diluted with 9.9 mL of fresh ethanol. The absorbance of the resulting
126 solution was measured at 275 nm using a spectrophotometer (Spekol 1500, Analytik Jena AG,
127 Jena, Alemania). Previously, known concentrations of thymol in ethanol were measured at this
128 wavelength to calculate a calibration curve. The encapsulation efficiency (EE%) was calculated
129 according to the following equation.

$$130 \quad \text{EE}\% = \frac{\text{thymol encapsulated}}{\text{thymol added in the DCM solution}} \times 100 \quad (1)$$

131

132 **2.4. Nanoparticle morphology**

133 A drop of the nanoparticle solution was placed on a copper grid and negatively stained with a
134 drop of phosphotungstic acid solution 2% (w/v). The micrographs were obtained using a

135 transmission electron microscope (TEM, JEOL-2000 EX-II, Tokyo, Japan) operated at 200 kV.
136 Furthermore, micrographs obtained using a scanning electron microscopy (SEM, JSM-6610LV,
137 JEOL, USA) were also performed. In this case, a drop of the sample was dried on a glass
138 microscope slide and coated with gold. The surface morphology of the nanoparticles was
139 observed at 20 kV.

140 **2.5. Nanoparticle storage stability at various pHs**

141 A freshly prepared solution of nanoparticles was centrifuged at 13000 rpm for 20 minutes and
142 the supernatant was discarded. The sediment, which contains the nanoparticles, was
143 resuspended in a buffer solution at pH 4.0 (phosphate-citrate), or at pH 7.0 (Trizma®), or at pH
144 9.0 (sodium carbonate-bicarbonate) and stored at 5 °C. The buffer concentration was 0.01 M in
145 all cases. Periodically, the average size of the nanoparticles and the thymol content were
146 measured.

147

148 **2.6. Thermogravimetric analysis (TGA)**

149 The samples tested were lyophilized for 24 hours whilst applying a pressure of 0.33 mbar. The
150 TGA curves were carried out in an SDTA851e TGA analyser (Mettler-Toledo, Switzerland) from
151 30 °C to 700 °C, under a nitrogen atmosphere. The heating rate was 10 °C/min. In this case, four
152 samples were tested: the nanoparticles loaded with thymol; the nanoparticles prepared as
153 described in section 3.2, but without the addition of thymol (unloaded nanoparticles); the
154 thymol and the PLA.

155 **2.7. *In vitro* thymol release profile**

156 To evaluate the thymol release profile, 10 mL of a freshly prepared solution of nanoparticles was
157 placed in a dialysis tube of 10 kDa MWCO, which was placed in a thermostatically controlled, 15
158 L capacity water bath (ref. 3001373, J. P. Selecta, Barcelona, Spain). The water in the bath was
159 under agitation due to a water stream provided by a pump. Several temperatures were tested,
160 and periodically one aliquot of 0.5 mL was taken from the dialysis tube and the thymol content
161 in the nanoparticles measured. To characterise the thymol release profile, the data obtained
162 were modelled using a first order equation (eq. 2) and the Korsmeyer-Peppas equation (eq. 3)
163 (Siepmann and Peppas, 2001).

164

$$165 \quad \frac{M_t}{M_\infty} = 1 - e^{-kt} \quad (2)$$

$$166 \quad \frac{M_t}{M_\infty} = k \times t^n \quad (3)$$

167

168 Where $\frac{Mt}{M\infty}$ is the accumulated percentage of thymol released at each time (t), k is the release
169 constant of thymol and n is the diffusion exponent that characterises the release mechanism of
170 the thymol.

171

172

173 **2.8. Nanoparticle antimicrobial properties**

174

175 To compare the antimicrobial properties of thymol and the nanoparticles loaded with thymol,
176 apple pieces weighing 1 g were inoculated with the non-pathogenic *E. coli* CECT 101 strain. This
177 strain was incubated at 30 °C for 48 hours using NB medium supplemented with 2% agar. To
178 prepare the liquid inoculum, *E. coli* was incubated in NB liquid medium for 10 hours, at 30 °C
179 with orbital stirring (250 rpm).

180 For all these treatments, each piece of apple was inoculated with 100 µL of *E. coli* and left for 2
181 minutes. The *E. coli* concentration used for this experiment was 10⁵ UFC/mL, which might be
182 considered high, but the strong antimicrobial properties of thymol made it necessary so as to be
183 able to detect variation in the ability to decrease *E. coli* growth on the apple pieces between
184 different preparations. After the inoculation, the apple pieces were submerged for 1.5 minutes
185 in 5 mL of an aqueous solution that contained thymol or nanoparticles loaded with thymol. To
186 solubilise the thymol, crystals of this active agent were added to distilled water at a
187 concentration of 2 mg/mL, stirred overnight and filtered using nº1 Whatman paper. The
188 concentration of dissolved thymol was determined by mixing 0.1 mL of this filtered solution with
189 9.9 mL of ethanol and measuring the absorbance at 275 nm, in accordance with the
190 methodology described in section 2.3. To investigate the antimicrobial effect of this solution,
191 three thymol concentrations were tested: 0.94 mg/mL, which corresponds to the maximum
192 concentration of thymol dissolved in water, 0.5 mg/mL and 0.1 mg/mL. The same concentrations
193 of thymol were used for the nanoparticle samples. After the treatment, the apple pieces were
194 hermetically closed in polyethylene boxes and stored at 5 °C until their analysis. To follow the
195 growth of the *E. coli* on the apple surface, samples were taken at different times and mixed with
196 9 mL of NaCl 0.7%. Then, the samples were homogenised using a stomacher and cultured in NB-
197 agar medium. After 24 hours of incubation at 30 °C the *E. coli* colonies were counted and the
198 results obtained expressed as log₁₀ UFC/g.

199 **2.9. Statistical analysis**

200 Experiments were performed in triplicate and are shown as the mean value ± standard deviation
201 of three independent experiments (n = 3). Least significant differences (LSD) were calculated by

202 Fisher's test to determine significant differences between the tested samples. These analyses
203 were performed using the statistical software Statgraphics® V.15.2.06.

204

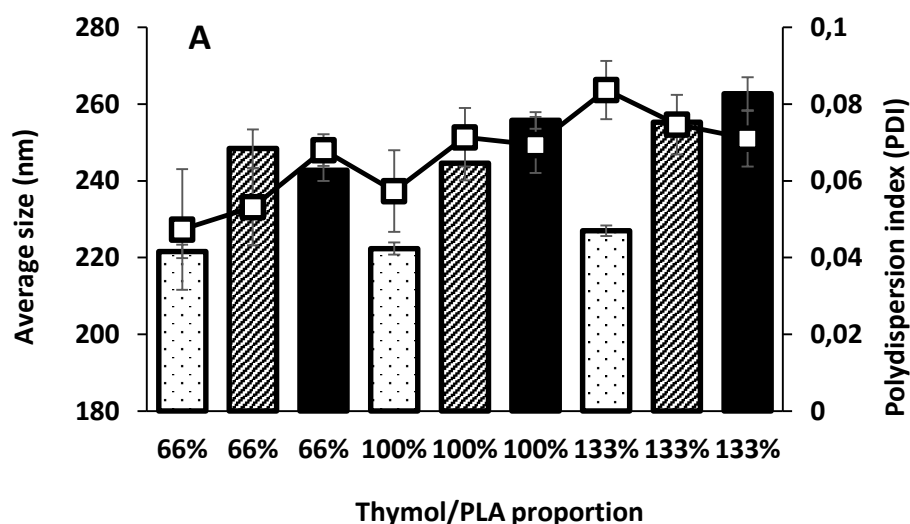
205 **3. Results**

206 **3.1. Size, polydispersity index, thymol recovered and encapsulation efficacy of the** 207 **nanoparticles prepared**

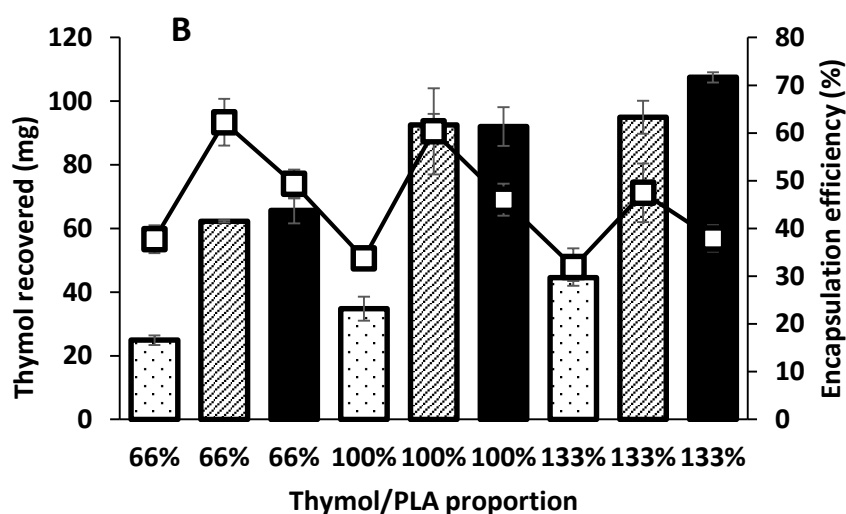
208 There are several parameters that could have a significant effect on the preparation of these
209 nanoparticles and have the capacity to modify their average size and the efficiency with which
210 they encapsulate thymol. In this sense, the variables which should be considered would include
211 the amount of DCM and water, the time and type of stirring used to obtain the emulsion
212 (ultrasounds or mechanical stirring), the amount of energy applied during the process, the type
213 and concentration of surfactant used to stabilise the emulsion, and the amounts of PLA and of
214 thymol. In our previous tests it was observed that, among all these parameters, variations in
215 the PLA and thymol concentrations produced changes in the properties of the nanoparticles in
216 a meaningful and straightforward way, and for this reason they were considered to be key
217 variables for this process.

218 Figure 1A indicates the average size of the prepared nanoparticles and their PDI, whilst in Figure
219 1B the amount of thymol encapsulated and the encapsulation efficiency are shown. According
220 to Figure 1A, these values suggest that, in broad terms, the higher the concentration of PLA in
221 the organic phase, the greater is the average size of the nanoparticles obtained. A similar trend
222 was observed when the amount of PLA was kept constant and the concentration of thymol was
223 increased. The latter effect was particularly pronounced in the 200 mg PLA samples.
224 Furthermore, in all cases the PDI values obtained were low enough to be considered satisfactory,
225 being even lower than those obtained by other authors in the preparation of similar PLA
226 nanoparticles (Roussaki et al., 2014; Wrona et al., 2017). As regards Figure 1B, the thymol
227 recovered from the nanoparticles followed a similar trend to the average size, in that increasing
228 the concentration of PLA and thymol led to an increase in the amount of thymol recovered.
229 However, the encapsulation efficiency showed a different trend to the recovered thymol
230 parameter, and the highest values obtained were from the 150 mg PLA preparations. In this
231 case, the 100 mg PLA preparations showed the lowest encapsulation efficiency values, probably
232 because the amount of PLA was low enough to produce nanoparticles with low internal density
233 and high porosity, which were incapable of retaining the thymol. In the case of the 200 mg PLA
234 nanoparticles, the density effect may have been reversed, and so, due to their high density, most
235 of the nanoparticles could have precipitated out by the end of the last centrifugation (5000 rpm,
236 4 min.), which was carried out in accordance with the preparation methodology described in the
237 materials and method section.

238 Taking into account all these results, and although the concentration of thymol and PLA
 239 produced variations in the size of the nanoparticles, in all the tested preparations this parameter
 240 was maintained within the 220 - 260 nm range. Since this could be considered a narrow range,
 241 it might be more effective to optimize the encapsulation efficiency in order to prevent loss of
 242 reagent and to increase the amount of thymol recovered. From the results shown in Figure 1B,
 243 the best preparation was seen to be that obtained using PLA and thymol concentrations of 150
 244 mg. Furthermore, the PLA concentration resulted more relevant than the thymol concentration
 245 to maximize the efficacy of encapsulation parameter.



246



247

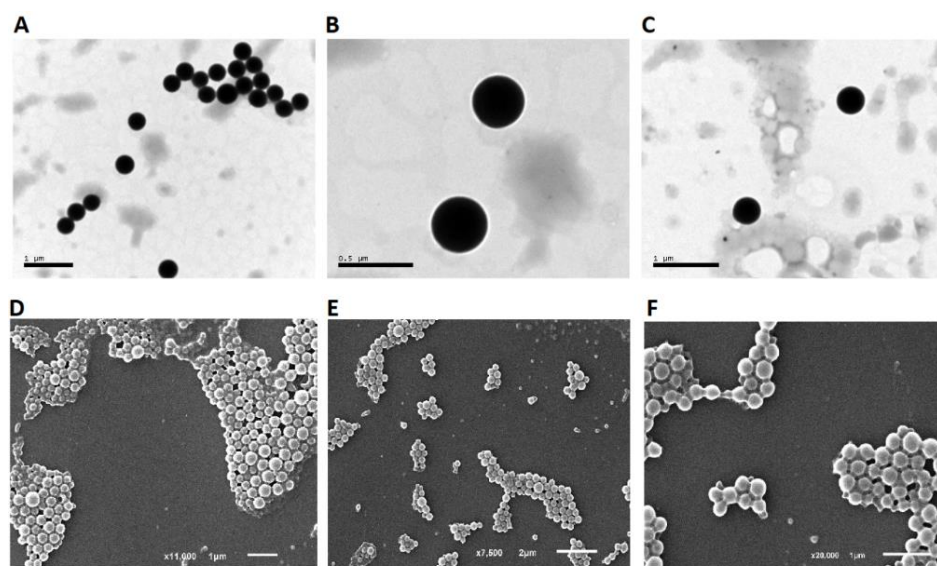
248 Figure 1. Parameters of interest for the characterisation of the nanoparticle preparations with
 249 respect to the PLA and thymol concentrations. Dotted bars correspond to the nanoparticles
 250 prepared using 100 mg de PLA, striped bars 150 mg of PLA and solid bars 200 mg of PLA. A:
 251 Average size (bars) and polydispersity index (line) of the nanoparticles prepared. B: Thymol
 252 recovered (bars) and encapsulation efficiency (line) of the nanoparticles prepared.

253

254 **3.2. Nanoparticle morphology**

255 The TEM and SEM micrographs of the nanoparticles prepared with 150 mg of PLA and several
256 concentrations of thymol are shown in Figure 2. In all the cases, spheres with a smooth surface
257 were observed. The size of the nanoparticles varied between 240 and 260 nm, corroborating
258 the values obtained by DLS provided in section 3.1. The morphology of the nanoparticles
259 prepared using proteins or polysaccharides is not usually so regular, and may have a rougher
260 appearance, which could have some influence on the release profile of the active agent.
261 Wattanasatcha et al. (2012) produced nanoparticles of ethylcellulose/methylcellulose loaded
262 with thymol and with an almost spherical morphology. Similar results were obtained by Xue et
263 al. (2014) preparing nanodispersions of lecithin, gelatin and thymol.

264



265
266 Figure 2. TEM (A, B, C) and SEM (C, D, E) micrographs of the nanoparticles prepared using 150
267 mg of PLA and 100 mg (A, D), 150 mg (B, E) and 200 mg (C, F) of thymol.

268 269 **3.3. Nanoparticle storage stability at several pHs**

270 The storage stability of the nanoparticles was tested at several pHs. For this purpose, the
271 average size and the thymol encapsulated were evaluated every 10 days for 40 days. The results
272 obtained are shown in Table 2. In all the tested samples, during a period of 40 days no changes
273 were detected in the size of the nanoparticles at any pH. As regards the thymol encapsulated,
274 at basic pH a slight decrease in this parameter was detected. In the case of the nanoparticles
275 stored at pH 7.0 and 4.0, this decrease was even less pronounced. This could be due to the
276 deprotonation of the phenolic hydroxyl group of the thymol at basic pH (Wu et al., 2012), which
277 would increase its solubility in water, therefore enhancing the movement of the active agent
278 from the nanoparticle to the aqueous medium. In any case, the decrease detected in the thymol
279 loaded within the nanoparticles in 40 days can be considered low at all the pHs tested. Finally,
280 it should be remembered that the encapsulation of thymol in protein-based nanoparticles is
281 usually pH-dependent, since the proteins tend to aggregate or solubilize at a specific range of

282 pH. In this case, the PLA nanoparticles do not exhibit this inconvenience and can be used over
 283 a wide range of pHs.

284

285 Table 2. Storage stability of the nanoparticles loaded with thymol at several pHs for 40 days.

	Average size (nm)					Thymol encapsulated (%)				
	Day 1	Day 10	Day 20	Day 30	Day 40	Day 1	Day 10	Day 20	Day 30	Day 40
pH 4.0	241.3 ±	242.7 ±	240.15 ±	239.1 ±	238.0 ±	100 ^a	95.8 ±	96.4 ±	96.0 ±	96.5 ±
	1.3 ^a	2.7 ^a	0.2 ^a	2.2 ^a	2.5 ^a		0.6 ^b	0.6 ^b	1.0 ^b	1.0 ^b
pH 7.0	238.7 ±	241.0 ±	238.9 ±	238.1 ±	239.5 ±	100 ^a	98.2 ±	98.9 ±	98.0 ±	97.3 ±
	1.3 ^a	0.5 ^a	1.8 ^a	1.5 ^a	1.2 ^a		0.7 ^b	0.8 ^b	1.2 ^b	0.6 ^b
pH 9.0	238.6 ±	240.8 ±	238.8 ±	240.4 ±	239.0 ±	100 ^a	96.7 ±	95.5 ±	96.2 ±	92.2 ±
	0.1 ^a	1.5 ^a	1.8 ^a	2.0 ^a	1.0 ^a		0.8 ^b	1.3 ^b	0.9 ^b	1.4 ^c

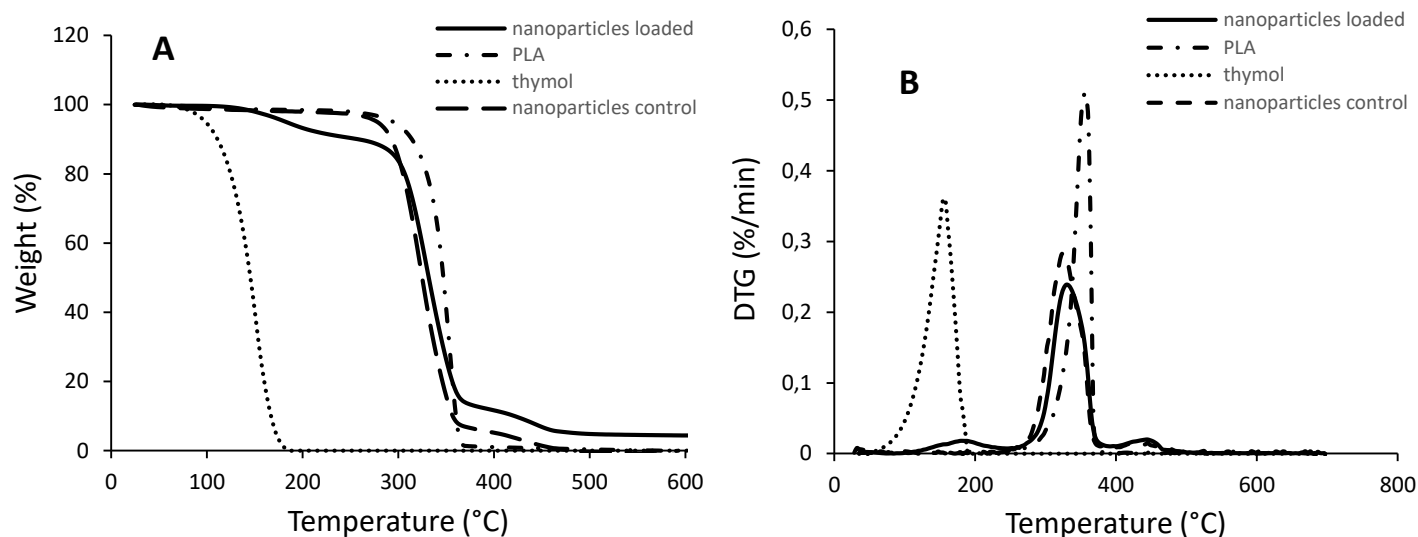
286 Different letters in the same row indicate significant differences (P<0.05).

287

288 3.4. TGA analysis

289 The TGA analysis of the lyophilized nanoparticles prepared using 150 mg of PLA and the same
 290 amount of thymol, the nanoparticles control without thymol, the reactive thymol and the PLA
 291 are shown in Figure 3A. The derivative of the TGA curves (DTG) obtained are shown in Figure 3B.
 292 In these Figures it can be observed that the pure thymol is degraded completely in one single
 293 stage and over the temperature range 65-190 °C, showing a maximum rate of degradation at
 294 158 °C. The PLA was degraded in a similar way as the thymol but at temperatures between 280
 295 and 370 °C. The nanoparticles control, without thymol, showed a degradation curve similar to
 296 that found for the pure PLA, but divided into two stages. The first of them corresponds to PLA
 297 degradation, from 280 °C to 370 °C and the second one, from 390 °C to 470 °C, corresponds to
 298 PVA degradation (Yu et al., 2003). The degradation of the nanoparticles loaded with thymol was
 299 produced in three stages (Figure 3B). While the second and third stages are similar to those
 300 found for the control nanoparticles, the first stage could be attributed to the degradation of
 301 thymol, but it is offset to the right in comparison with that found for the pure thymol. In fact,
 302 this first degradation stage takes place from 120 °C to 250 °C, with a maximum degradation rate
 303 at 182 °C. This increase in the temperature of degradation of the encapsulated thymol could
 304 occur due to its inclusion in the nanoparticles, which provide a protective environment.
 305 Furthermore, it is significant that the amount of thymol in these nanoparticles is only around
 306 10% of the weight of the lyophilized nanoparticles. This decrease in the thymol content could
 307 be due to the evaporation of thymol during the lyophilization process, since this active agent is

308 a highly volatile essential oil and the drying process involves the application of low pressures for
309 a relatively long time.



311 Figure 3. TGA (A) and DTG (B) curves of the nanoparticles loaded with thymol, the nanoparticles
312 control without thymol, the reactive thymol and the PLA.

313 3.5. *In vitro* thymol release profile

314 The thymol release profiles of the loaded (150 mg of PLA and of thymol) nanoparticles at
315 different temperatures were determined and are shown in Figure 4. Although this type of
316 experiment has been designed principally to investigate the behaviour of injectable
317 encapsulated drugs in the bloodstream, it can also provide valuable information about the state
318 of the active agent inside the nanoparticle matrix and could provide evidence about possible
319 interactions between the nanoparticle polymers and the active agent. According to this Figure,
320 the thymol diffuses rapidly from the nanoparticles into the aqueous medium at 35 °C, releasing
321 93% of the active agent in 6 h. In the same time, if the temperature is lowered to 22 °C, 80% of
322 the thymol is released. However, at 15 and 5 °C, the release of thymol over 6 hours decreases
323 to 60%. As was to be expected, the rate of thymol release is temperature-dependent. Both at
324 35 and 22 °C the release of thymol for the first 2 hours is fast, and then a slight decrease in this
325 release rate was detected. This first burst effect in 2 hours could be due to the release of the
326 thymol adhered to the surface of the nanoparticles and to the thymol that is within the
327 nanoparticles, but in the more external layers (Yadav and Sawant, 2010). The geometry of the
328 nanoparticles and their high surface/volume ratio could be the reason for this first fast release.
329 From this point, the thymol released came from the inner layers of the nanoparticles.

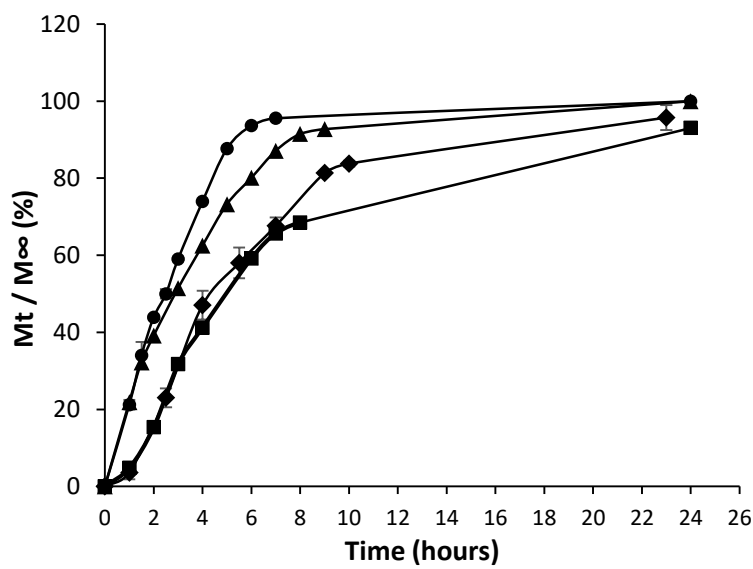
330 Furthermore, during the first hour at 15 and 5 °C there is a slight delay in the thymol release.
331 This slow release could be due to the presence of free thymol remaining in the solution
332 containing the nanoparticles. At the beginning of the test this thymol would be in the process of
333 diffusing out of the dialysis tube, whereas at the highest temperatures tested, the thymol
334 cleared quickly from the dialysis tube. Once the thymol excess disappears from the dialysis tube,

335 the active agent is released quickly between the first and the fourth hour, in the case of the 15
336 °C experiment, and between the first and third hour when the temperature is lowered to 5 °C.
337 Then, the thymol in the inner layers of the nanoparticles is also released, but at a lower speed.
338 In any case, and bearing in mind that the antimicrobial and antioxidant properties of the thymol
339 are concentration-dependent, this initial burst effect is desirable, since it allows an initial
340 increase in the amount of free thymol in the medium.

341 There are several empirical models that can easily be applied to release profiles similar to those
342 shown in Figure 4 and that have been widely reported in bibliography. In this case, the
343 Korsmeyer-Peppas model was used, and the results obtained are shown in Table 3. To apply this
344 model, only the data from the release curve up to 60% thymol release were considered
345 (Siepmann and Peppas, 2012). Furthermore, neither the first hour in the experiments at 35 and
346 22 °C, nor the first two hours in those at 15 and 5 °C were considered. This omission was due to
347 the distortion produced in the model by the burst effect at the two highest temperatures tested,
348 and the delay detected in the thymol release at the two lowest temperatures. In this model, the
349 value of the exponent “n” could be used to interpret, to some extent, the process of the
350 mobilization of the thymol from the interior of the nanoparticle to the aqueous medium. Thus,
351 if “n” is equal to 0.43, the diffusion of the active agent follows Fick’s law. On the other hand, if
352 the “n” value varies between 0.43 and 0.85, then the transport mechanism is catalogued as
353 anomalous, being a mixture of Fickian diffusion and the movement of thymol produced by
354 swelling of the nanoparticle. If alternatively, the value of “n” is equal to 0.85, then the transport
355 is caused mainly by the nanoparticle swelling (Ritger and Peppas, 1987). Bearing this in mind
356 and referring to Table 3, in all the cases in this experiment the mechanism of transport is
357 anomalous, except at 5 °C, where due to the decrease in the temperature, the diffusion
358 mechanism was hindered and the transport produced by the nanoparticle swelling becoming
359 more important.

360 In Table 3 are also shown the first order kinetic equation parameters obtained from the
361 experimental data. These results showed that in all the cases the thymol release can be adjusted
362 to this type of kinetic with a high coefficient of determination (R^2), which suggests that this
363 release is dependent on the thymol concentration. Furthermore, and as was expected, the “k”
364 value decreased when the temperature also decreased, showing that the release of this active
365 agent at low temperatures is slower in comparison with the same release at high temperatures.

366



367

368 Figure 4. Thymol release from the nanoparticles prepared using 150 mg of PLA and 150 mg of
 369 thymol at 35 °C (circles), 22 °C (triangles), 15 °C (rhombi), and at 5 °C (squares).

370

371

372 Table 3. Parameters of interest obtained from Figure 4.

	First order		Korsmeyer-Peppas	
	R ²	k	R ²	n
35 °C	0.94	0.40	0.99	0.77
22 °C	0.98	0.28	0.99	0.67
15 °C	0.97	0.17	0.99	0.60
5 °C	0.97	0.14	0.98	0.85

373

374

375

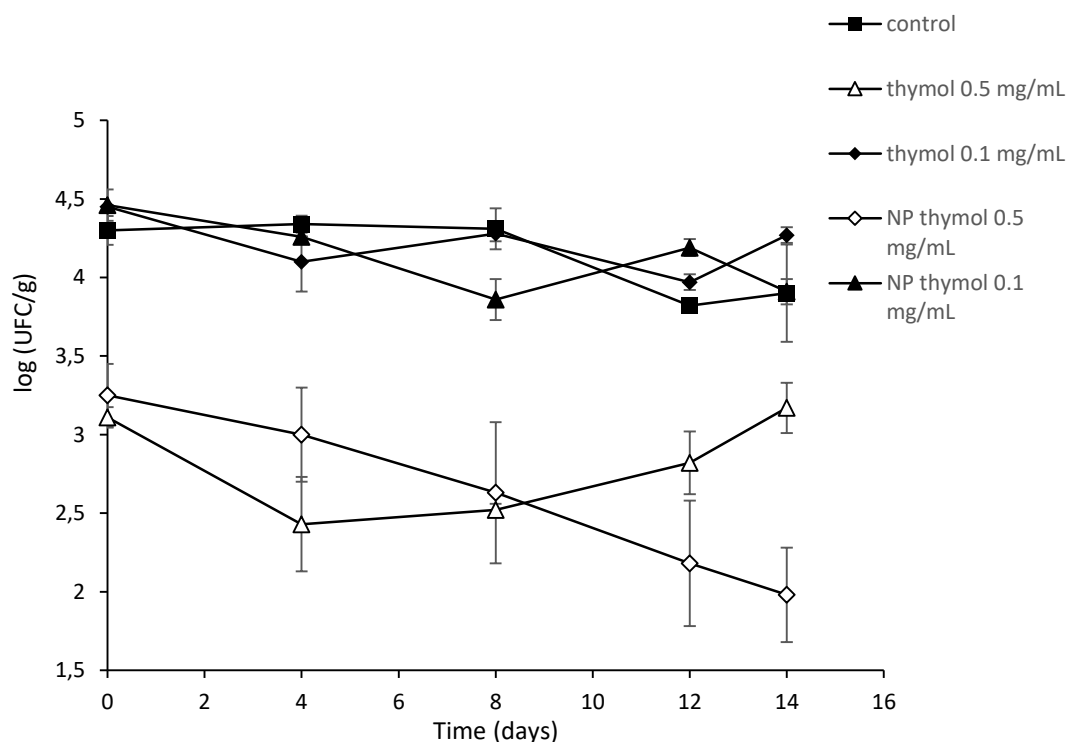
376

377 3.6. antimicrobial properties of the nanoparticles

378 In Figure 5 is shown the effect of the aqueous solution with free thymol and the thymol
 379 encapsulated in nanoparticles on *E. coli* growth. In the samples treated with free and
 380 encapsulated thymol at 0.94 mg/mL, it was not possible to detect *E. coli* growth during the 14
 381 days of treatment, so the thymol at this concentration was able to kill all the bacterial population
 382 inoculated. On the other hand, the solutions with a thymol concentration of 0.1 mg/mL showed

383 a behaviour similar to that found in the control sample, it being impossible to detect differences
 384 between the encapsulated and non-encapsulated thymol. Therefore, the lowest thymol
 385 concentration tested did not have any effect on the growth of *E. coli*. However, in the samples
 386 treated with 0.5 mg/mL of thymol it was possible to detect a difference between the
 387 nanoparticles and the free thymol. While the free thymol was seen to be more effective than
 388 the nanoparticles in the initial days of the experiment, the encapsulated thymol produced a
 389 continuous decrease in *E. coli* growth during the 14 days of the experiment, proving to be more
 390 effective than the free thymol in the long-term. This could be due to the nanoparticles providing
 391 an environment that protects the thymol from evaporation, maintaining its effect for longer.

392 The superficial application of the nanoparticles loaded with thymol on the surface of a solid
 393 food could be a more realistic use for them than the typical applications found in the
 394 bibliography, which are mainly focused on the antibacterial properties of nanoparticles in liquid
 395 foods (Chen et al., 2014; Chen et al., 2015; Pan et al., 2014; Shah et al., 2012). Although from a
 396 scientific point of view, the use of liquid food to study the antibacterial properties of thymol-
 397 loaded nanoparticles is very interesting, in a practical way it requires a homogeneous dispersion
 398 of the thymol throughout the volume of the liquid, and in this case the flavour of the thymol
 399 could affect the organoleptic properties of the product, even though this active agent is
 400 encapsulated. However, the use of these nanoparticles to protect the surface of solid food
 401 requires only its immersion in a nanoparticle suspension, which limits the contact of the product
 402 with the active agent while the nanoparticles maintain their capacity to protect the thymol and
 403 release it over time.



404

405 Figure 5. Growth of *E. coli* CECT 101 on apples treated with solutions containing free thymol
 406 and nanoparticles loaded with thymol.

407

408 **4. Conclusions**

409 In the tests performed using different PLA and thymol concentrations, the amount of PLA was
410 found to be a key parameter to optimize the preparation of the thymol-loaded nanoparticles.
411 These nanoparticles exhibited a spherical morphology, with a smooth surface and high storage
412 stability over a wide range of pHs. Precisely, this stability at acidic and basic pHs could be
413 considered an advantage in favour of these PLA nanoparticles when compared to those
414 prepared using proteins and/or carbohydrates. Furthermore, their regular morphology and the
415 homogenous arrangement of the active agent in the core are other relevant features that other
416 biopolymer-based nanoparticles lack, and that have an important effect on the way the
417 nanoparticles release the active agent. However, as can be seen from the TGA curves of the
418 lyophilized PLA nanoparticles shown previously, a large proportion of the thymol evaporated
419 during the lyophilization process, although this inconvenience could be compensated by the
420 great stability of the nanoparticles in an aqueous suspension. Finally, using apple pieces
421 inoculated with *E. coli* as a real food model, the PLA nanoparticles showed the capacity to
422 maintain the thymol activity for 14 days, probably limiting its evaporation from the wet surface
423 of the apple and favouring its release over time. The use of thymol-loaded nanoparticles to
424 protect the surface of solid foods could be a more realistic use for them than their incorporation
425 in liquid foods, since the first use limits the amount of thymol necessary to produce its
426 antibacterial effect, minimising the strong flavour of the thymol.

427

428 **5. References**

429

430 Andrade-Ochoa, S., Nevárez-Moorillón, G.V., Sánchez-Torres, L.E., Villanueva-García, M.,
431 Sánchez-Ramírez, B.E., Rodríguez-Valdez, L.M., Rivera-Chavira, B.E., (2015). Quantitative
432 structure-activity relationship of molecules constituent of different essential oils with
433 antimycobacterial activity against *Mycobacterium tuberculosis* and *Mycobacterium bovis*. *BMC*
434 *complementary and alternative medicine* 15(1), 332.

435 Chen, H., Davidson, P.M., Zhong, Q., (2014). Impacts of sample preparation methods on
436 solubility and antilisterial characteristics of essential oil components in milk. *Applied and*
437 *Environmental Microbiology* 80(3), 907-916.

438 Chen, H., Zhang, Y., Zhong, Q., (2015). Physical and antimicrobial properties of spray-dried zein-
439 casein nanocapsules with co-encapsulated eugenol and thymol. *Journal of Food Engineering*
440 144, 93-102.

441 da Rosa, C.G., de Oliveira Brisola Maciel, M.V., de Carvalho, S.M., de Melo, A.P.Z., Jummes, B.,
442 da Silva, T., Martelli, S.M., Villetti, M.A., Bertoldi, F.C., Barreto, P.L.M., (2015). Characterization
443 and evaluation of physicochemical and antimicrobial properties of zein nanoparticles loaded

444 with phenolics monoterpenes. *Colloids and Surfaces A: Physicochemical and Engineering*
445 *Aspects* 481, 337-344.

446 Džamić, A., Nikolić, B., Giweli, A., Mitić-Ćulafić, D., Soković, M., Ristić, M., Knežević-Vukčević, J.,
447 Marin, P., (2015). Libyan *Thymus capitatus* essential oil: antioxidant, antimicrobial, cytotoxic and
448 colon pathogen adhesion-inhibition properties. *Journal of applied microbiology* 119(2), 389-399.

449 Hernández-Hernández, E., Regalado-González, C., Vázquez-Landaverde, P., Guerrero-Legarreta,
450 I., García-Almendárez, B.E., (2014). Microencapsulation, chemical characterization, and
451 antimicrobial activity of Mexican (*Lippia graveolens* HBK) and European (*Origanum vulgare* L.)
452 oregano essential oils. *The Scientific World Journal* 2014.

453 Huang, Q., (2012). *Nanotechnology in the food, beverage and nutraceutical industries*. Elsevier.

454 Lee, B.K., Yun, Y., Park, K., (2016). PLA micro- and nano-particles. *Advanced Drug Delivery*
455 *Reviews* 107, 176-191.

456 Li, K.-K., Yin, S.-W., Yang, X.-Q., Tang, C.-H., Wei, Z.-H., (2012). Fabrication and characterization
457 of novel antimicrobial films derived from thymol-loaded zein–sodium caseinate (SC)
458 nanoparticles. *Journal of Agricultural and Food Chemistry* 60(46), 11592-11600.

459 Mastelić, J., Jerković, I., Vinković, M., Džolić, Z., Vikić-Topić, D., (2004). Synthesis of selected
460 naturally occurring glucosides of volatile compounds. Their chromatographic and spectroscopic
461 properties. *Croatica chemica acta* 77(3), 491-500.

462 Nair, L.S., Laurencin, C.T., (2005). Polymers as biomaterials for tissue engineering and controlled
463 drug delivery, *Tissue engineering I*. Springer, pp. 47-90.

464 Pan, K., Chen, H., Davidson, P.M., Zhong, Q., (2014). Thymol nanoencapsulated by sodium
465 caseinate: physical and antilisterial properties. *Journal of Agricultural and Food Chemistry* 62(7),
466 1649-1657.

467 Piccaglia, R., Marotti, M., Giovanelli, E., Deans, S., Eaglesham, E., (1993). Antibacterial and
468 antioxidant properties of Mediterranean aromatic plants. *Industrial Crops and Products* 2(1), 47-
469 50.

470 Ritger, P.L., Peppas, N.A., (1987). A simple equation for description of solute release I. Fickian
471 and non-fickian release from non-swellable devices in the form of slabs, spheres, cylinders or
472 discs. *Journal of Controlled Release* 5(1), 23-36.

473 Roussaki, M., Gaitanarou, A., Diamanti, P.C., Vouyiouka, S., Papaspyrides, C., Kefalas, P., Detsi,
474 A., (2014). Encapsulation of the natural antioxidant aureusidin in biodegradable PLA
475 nanoparticles. *Polymer Degradation and Stability* 108, 182-187.

476 Shah, B., Davidson, P.M., Zhong, Q., (2012). Nanocapsular dispersion of thymol for enhanced
477 dispersibility and increased antimicrobial effectiveness against *Escherichia coli* O157: H7 and
478 *Listeria monocytogenes* in model food systems. *Applied and Environmental Microbiology*
479 78(23), 8448-8453.

480 Siepmann, J., Peppas, N., (2012). Modeling of drug release from delivery systems based on
481 hydroxypropyl methylcellulose (HPMC). *Advanced Drug Delivery Reviews* 64, 163-174.

482 Siepmann, J., Peppas, N.A., (2001). Modeling of drug release from delivery systems based on
483 hydroxypropyl methylcellulose (HPMC). *Advanced Drug Delivery Reviews* 48(2), 139-157.

484 Stahl-Biskup, E., Sáez, F., (2003). *Thyme: the genus Thymus*. CRC Press.

485 Wattanasatcha, A., Rengpipat, S., Wanichwecharungruang, S., (2012). Thymol nanospheres as
486 an effective anti-bacterial agent. *International Journal of Pharmaceutics* 434(1–2), 360-365.

487 Wrona, M., Cran, M.J., Nerín, C., Bigger, S.W., (2017). Development and characterisation of
488 HPMC films containing PLA nanoparticles loaded with green tea extract for food packaging
489 applications. *Carbohydrate Polymers* 156, 108-117.

490 Wu, Y., Luo, Y., Wang, Q., (2012). Antioxidant and antimicrobial properties of essential oils
491 encapsulated in zein nanoparticles prepared by liquid–liquid dispersion method. *LWT - Food*
492 *Science and Technology* 48(2), 283-290.

493 Xue, J., Zhong, Q., (2014). Blending lecithin and gelatin improves the formation of thymol
494 nanodispersions. *Journal of Agricultural and Food Chemistry* 62(13), 2956-2962.

495 Yadav, K.S., Sawant, K.K., (2010). Formulation optimization of etoposide loaded PLGA
496 nanoparticles by double factorial design and their evaluation. *Current drug delivery* 7(1), 51-64.

497 Yu, Y.-H., Lin, C.-Y., Yeh, J.-M., Lin, W.-H., (2003). Preparation and properties of poly (vinyl
498 alcohol)–clay nanocomposite materials. *Polymer* 44(12), 3553-3560.

499 Zhang, Y., Niu, Y., Luo, Y., Ge, M., Yang, T., Yu, L., Wang, Q., (2014). Fabrication, characterization
500 and antimicrobial activities of thymol-loaded zein nanoparticles stabilized by sodium caseinate–
501 chitosan hydrochloride double layers. *Food Chemistry* 142, 269-275.

502